Gene Expression Time Course in the Human Skin during Elicitation of Allergic Contact Dermatitis

Malene B. Pedersen[1], Lone Skov[2], Torkil Menné[2], Jeanne D. Johansen[1] and Jørgen Olsen[3]

Genes involved in the inflammatory response resulting in allergic contact dermatitis (ACD) are only partly known. In this study, we introduce the use of high-density oligonucleotide arrays for gene expression profiling in human skin during the elicitation of ACD. Skin biopsies from normal and nickel-exposed skin were obtained from seven nickel-allergic patients and five nonallergic controls at four different time points during elicitation of eczema. Each gene expression profile was analyzed by hybridization to high-density oligonucleotide arrays. Cluster analysis of 74 genes found to be differentially expressed in the patients over time revealed that the patient samples may be categorized into two groups: an early time-point group (no clinical reaction) and a late time-point group (clinical reaction). Bioinformatics analyses unraveled the potential involvement of signal transducers and activator of transcription and small/mothers against decepentaplegic (SMAD) transcription factors in the late time-point gene expression patterns. Concerning specific genes, the homeostatic chemokine CCL19 was unexpectedly found to be highly expressed in cells scattered in the deep dermis of the late time-point samples. Taken together, these findings suggest hitherto unknown roles of SMAD transcription factors and of CCL19 in the elicitation phase of ACD.

Journal of Investigative Dermatology advance online publication, 28 June 2007; doi:10.1038/sj.jid.5700902

INTRODUCTION

Allergic contact dermatitis (ACD), both occupational and nonoccupational, comprises a major health problem in the industrial world. The disease is characterized by local inflammation in the skin with particular involvement of the hands, feet, and face (Veien, 2006). Contact sensitizers or haptens are small molecules with a molecular weight of <700 Da (Scheynius, 1998). Common sensitizing haptens include metals, biocides/preservatives, fragrance chemicals, and dyes.

ACD is a type IV hypersensitivity mediated by activated allergen-specific T lymphocytes. ACD is the clinical manifestation and it is preceded by a sensitization phase, which is clinically silent. Much has been learned about ACD from studies using the rodent contact hypersensitivity (CHS) models. During sensitization, dendritic cells (DCs) that have taken up a hapten migrate to draining lymph nodes (LNs) where they mature, express costimulatory molecules, and present antigens to naïve CCR7-positive T cells (for reviews see Sebastiani *et al.* 2002; Wang *et al.*, 2003; Sanchez-Sanchez *et al.*, 2006). The CCR7-positive DCs as well as the naïve CCR7-expressing T cells are attracted to the LNs by homeostatic CCR7 ligands, chemokines CCL19 and CCL21, which are constitutively expressed in the LNs (Sebastiani *et al.*, 2002; Ebert *et al.*, 2005). When a sensitized person is exposed to the hapten, specific T cells are recruited by chemokines to the skin where the cells undergo extensive proliferation (Rustemeyer *et al.*, 2003). The activated T cells subsequently produce and release high levels of cytokines, thereby causing an inflammatory process leading to eczema. Interferon-γ is believed to be an important T-cell-derived cytokine with an effector function during the elicitation of ACD (Wang *et al.*, 2003). Given the complexity of the molecular mechanisms, studies of isolated genes are not, however, sufficient to give the complete picture of the pathogenesis of ACD. No human genome-wide gene expression analysis has yet been reported for the elicitation phase and in this study, we therefore introduce the use of DNA microarrays (Stoughton, 2005) into the investigation of gene expression changes in the skin during the elicitation of ACD. It was our purpose to provide first an overall insight into the biological processes and regulating transcription factors in the elicitation phase of ACD from bioinformatics analyses of the genome-wide expression data. Secondly, it was our purpose to identify new specific molecular details about the disease process.

[1]*The National Allergy Research Centre for Consumer Products, Gentofte Hospital, University of Copenhagen, Copenhagen, Denmark;* [2]*Department of Dermatology, Gentofte Hospital, University of Copenhagen, Copenhagen, Denmark and* [3]*Department of Cellular and Molecular Medicine, The Panum Institute, University of Copenhagen, Copenhagen, Denmark*

Correspondence: Dr Jørgen Olsen, Department of Cellular and Molecular Medicine, The Panum Institute Building 6.4., University of Copenhagen, DK- 2200 N, Denmark. E-mail: jolsen@imbg.ku.dk

Abbreviations: ACD, allergic contact dermatitis; ANOVA, analysis of variance; AP-2γ, activator protein 2γ; CA, correspondence analysis; CHS, contact hypersensitivity; DC, dendritic cells; LN, lymph nodes; RT-PCR, reverse transcription-PCR; SMAD, small/mothers against decepentaplegic; STAT, signal transducers and activator of transcription

Received 15 November 2006; revised 2 April 2007; accepted 6 April 2007

© 2007 The Society for Investigative Dermatology

RESULTS

Patch test results

In all eight nickel-allergic patients, an allergic reaction was elicited in response to nickel exposure. The visible allergic reaction appeared at the 48- and 96-hour time points. No visible eczema was observed in any patient at time point 0 and 7 hours. None of the six nonallergic controls had any visible reaction to the patch test with nickel sulfate. Skin biopsies were obtained at all four time points from all participating patients and controls.

Multivariate analysis reveals active biological processes during elicitation of ACD

RNA was extracted from the skin biopsies and a genome-wide gene expression analysis carried out using Affymetrix HGU 133 Plus 2.0 arrays. A one-way analysis of variance (ANOVA) was used to filter the dataset, resulting in a list of 678 probe sets reporting significantly different expression between the different groups of samples. The filtered probe sets were subjected to correspondence analysis (CA). CA reduced the 678 dimensions of the filtered dataset into two dimensions, retaining 82% of the variation present in the original filtered dataset. Thus, as a result of the dimension reduction, the first two axes catch up with the main variations in the original data. Figure 1 shows the score plot with the projections of each biopsy on the plane defined by the first and second CA axes. All the control biopsies are projected into one group located mainly in the upper left quadrant (negative values on the *x* axis and positive values on the *y* axis), whereas all patient biopsies are mainly distributed towards the upper and lower right quadrants (positive values on the *x* axis). The patient biopsies are further subdivided into two groups with different projections on the score plot. Late patient biopsies (48 and 96 hours) are projected to the far upper right quadrant, whereas the early patient biopsies (0 and 7 hours) are projected onto the lower right quadrant (negative values on the *y* axis and positive values on the *x* axis). Thus, Figure 1 reveals that the first axis distinguishes the skin from patients from the skin of control subjects, whereas the second axis separates skin in the late phase of the

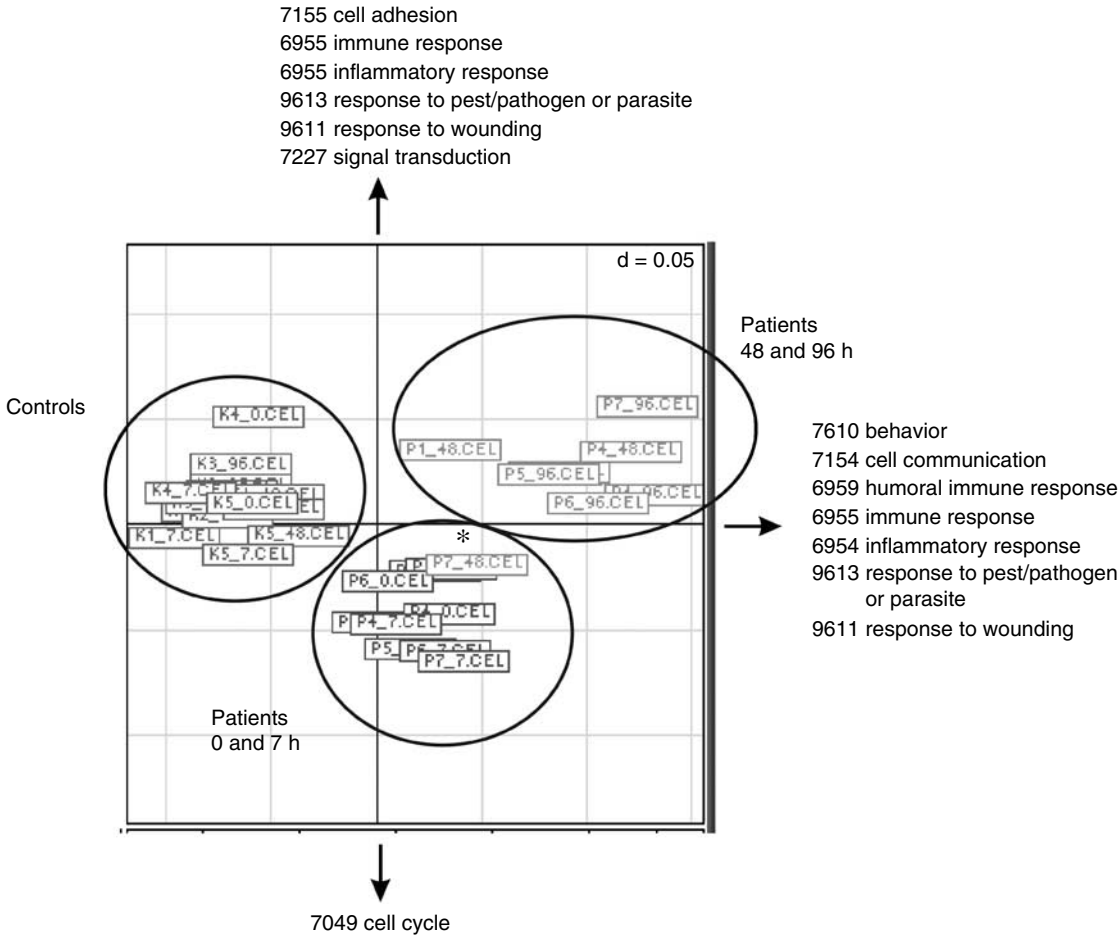

Figure 1. CA score plot. Plot of CA scores for the first and second CA axes. The projections of samples from control subjects, early (0 and 7 hours) patient samples and late (48 and 96 hours) patient samples are indicated by circles. A single late patient sample (P7_48.CEL) is projected together with the early patient group. The genes corresponding to the probe sets that define the positive and negative directions of the CA axis were analyzed for overrepresentation of terms for biological processes. Overrepresented Go IDs and terms (compared to the list of genes defining the other end of the same axis) are written in continuation of the axes.

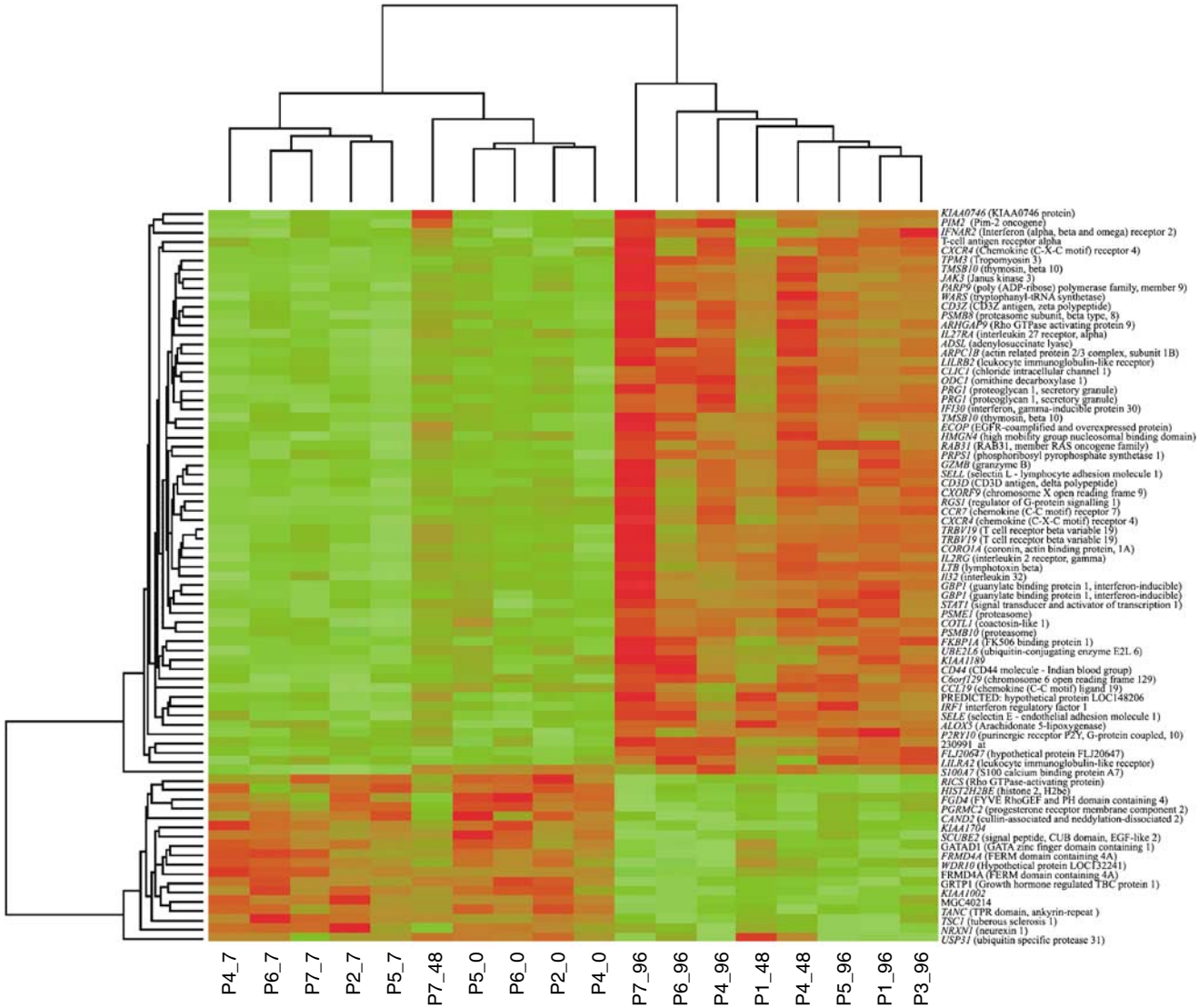

Figure 2. Hierarchical clustering of genes involved in the elicitation of ACD. Hierarchical clustering of the 74 probe sets that were significantly differentially expressed in at least one time point from the patient dataset, as determined by ANOVA. In the cluster diagram, each row represents a probe set and each column represents a biopsy. The number written immediately after the letter (*P* for patients) refers to the person and the number after the underscore refers to the time point. For example, P7_7 is data from patient no. 7 from the 7-hour time point. The colours indicate the experession level: red highest, green lowest.

elicitation of ACD from skin in the early phase of the elicitation of ACD.

The CA analysis was combined with a functional annotation analysis. The principle behind this analysis (Csillag *et al.*, 2007a) is to identify the probe sets that define the positive or negative directions of the axes and then identify annotation terms that are significantly overrepresented. The annotation terms are terms for biological processes defined by the Gene Ontology Consortium (Ashburner *et al.*, 2000). Terms for biological processes related to inflammation dominate in the annotation of the probe sets defining positive directions of both the first and second CA axes (Figure 1). In contrast, the term ''cell cycle'' was the only term found overrepresented in the annotation of the probe sets defining the negative directions of the CA axes. The lists of probe sets defining the four ends of the two axes were also analyzed for overrepresentation of potential transcription factor-binding sites in the promoters for the genes interrogated by the probe sets. Overrepresentation was only found in the promoters of the genes interrogated by probe sets defining the positive direction of the first CA axis. Potential binding sites for signal transducers and activator of transcription (STAT), activator protein 2γ (AP-2γ) and small/mothers against decepentaplegic (SMAD) transcription factors were found overrepresented (see Materials and Methods for details). It is therefore also noteworthy that probe sets for the STAT1 and the JAK3 kinase reported increased expression in the late time-point patient samples (Figure 2 and Table 1). STAT1 was also reported to display increased expression after hapten application in a recent DNA microarray-based study of CHS in the rat (Hartmann *et al.*, 2006).

Table 1. Genes significantly up- and downregulated during the elicitation of ACD

Gene symbol	Affymetrix Probe set ID	Expression intensity[1,2] 0 h	7 h	48 h	96 h
Immune response					
GZMB	210164_at	21±3	17±2	182±104	373±138
SELE	206211_at	38±7	41±20	447±195	654±177
RGS1	216834_at	27±1	9±1	74±39	206±88
LTB	207339_s_at	209±27	112±15	865±335	1,200±288
CCR7	206337_at	44±3	19±1	94±39	245±74
CCL19	210072_at	1,376±221	377±41	3,646±1,314	3,616±689
TRBV19	210915_x_at	110±15	81±15	310±48	476±100
TRBV19	213193_x_at	204±20	163±22	562±96	863±181
CD3D	213539_at	150±21	116±13	355±104	545±109
GBP1	202270_at	164±15	95±6	302±75	575±156
IL2RG	204116_at	102±15	69±6	279±58	312±71
GBP1	202269_x_at	210±31	155±5	434±115	693±120
IL32	203828_s_at	128±14	92±18	316±74	391±80
IFI30	201422_at	559±39	394±26	1,057±386	1,533±101
PSMB10	202659_at	192±12	156±23	321±60	433±26
LILRB2	207697_x_at	75±7	60±4	99±20	149±14
PSMB8	209040_s_at	284±21	263±13	414±55	485±21
PSME1	200814_at	905±30	827±17	1,172±88	1,236±50
LILRA2	211100_x_at	42±3	38±2	41±4	53±1
Cell mobility/cell adhesion					
SELL	204563_at	26±5	17±2	138±68	347±124
PARP9	223220_s_at	158±13	107±9	283±66	415±78
CORO1A	209083_at	178±25	151±23	457±120	592±91
ARPC1B	201954_at	632±40	526±38	1,057±301	1,296±79
RAB31	217764_s_at	369±14	383±10	565±43	678±50
Intracellular signaling/signal transduction					
CXCR4	217028_at	94±3	51±5	218±77	763±317
JAK3	227677_at	72±9	49±2	305±154	389±124
IL27RA	222062_at	38±7	18±2	91±31	111±26
CD3Z	210031_at	34±2	29±3	100±33	144±39
CXCR4	209201_x_at	51±7	40±2	93±19	227±56
STAT1	M97935_3_at	423±53	280±20	572±105	910±192
ECOP	208091_s_at	376±20	374±14	575±60	610±38
IFNAR2	204785_x_at	77±3	83±5	101±2	116±7
P2RY10	1553856_s_at	15±1	15±1	27±2	30±3
PGRMC2[3]	**201701_s_at**	**337±13**	**322±20**	**175±12**	**189±20**
TSC1	**209390_at**	**174±6**	**199±8**	**162±10**	**131±6**
Actin binding					
COTL1	224583_at	220±52	143±21	369±87	539±48
TMSB10	217733_s_at	5,701±368	5,477±248	7,775±777	9,228±640
TPM3	222976_s_at	2,100±83	1,865±17	2,761±438	3,353±119
FGD4	230559_x_at	12±1	10±1	8±0	8±0
Cellular metabolism					
IRF1	202531_at	111±10	99±6	240±49	302±29
WARS	200628_s_at	141±10	123±5	293±66	319±27

Table 1 continued on following page

Table 1. continued

Gene symbol	Affymetrix Probe set ID	Expression intensity[1,2] 0 h	7 h	48 h	96 h
ODC1	200790_at	379±33	346±23	713±146	830±82
LAP3	217933_s_at	655±44	525±22	979±227	1,251±135
UBE2L6	201649_at	280±22	226±6	338±8	491±53
PIM2	204269_at	48±1	46±4	75±13	78±4
ADSL	210250_x_at	321±4	293±10	422±63	501±23
PRPS1	209440_at	222±14	206±10	303±29	334±15
ALOX5	236199_at	26±1	29±1	33±2	40±1
IFT122	**241336_at**	**63±5**	**65±3**	**49±3**	**35±4**
CAND2	**213547_at**	**47±4**	**44±2**	**35±1**	**33±2**
GATAD1	**214718_at**	**231±10**	**214±9**	**157±24**	**127±9**
USP31	**227256_at**	**152±8**	**143±11**	**171±13**	**94±5**
Miscellaneous					
ARHGAP9	232543_x_at	53±3	46±4	120±36	128±17
S100A7	205916_at	3,105±385	237±57	3,223±858	3,773±1,189
FKBP1A	210187_at	24±1	20±2	35±5	60±9
CLIC1	208659_at	1,524±91	1,508±60	1,961±251	2,260±60
HMGN4	202579_x_at	475±25	437±21	616±55	638±25
SCUBE2	**219197_s_at**	**133±14**	**115±7**	**81±14**	**63±8**
HIST2H2BE	**202708_s_at**	**109±3**	**94±11**	**69±6**	**58±4**
RICS	**242196_at**	**27±1**	**24±2**	**17±2**	**16±0**
NRXN1	**209914_s_at**	**45±2**	**49±2**	**35±1**	**31±2**
Unknown function					
PRG1	201859_at	618±73	380±19	1,290±449	1,994±252
—	238725_at	59±6	59±5	210±65	232±52
CXorf9	204923_at	59±7	43±2	158±47	195±26
PRG1	201858_s_at	350±21	286±21	848±339	1,198±128
KIAA0746	212311_at	30±2	30±3	75±12	72±9
—	229221_at	36±2	31±2	57±18	76±8
FLJ20647	218802_at	155±5	157±6	204±41	283±8
C6orf129	225723_at	82±10	70±4	106±19	123±4
KIAA1189	231911_at	11±1	10±0	11±0	15±1
—	224343_x_at	12±0	12±0	17±1	18±1
—	230991_at	12±1	13±0	14±1	17±0
FRMD4A	**1560031_at**	**272±6**	**305±37**	**204±23**	**122±10**
FRMD4A	**208476_s_at**	**168±6**	**219±21**	**135±15**	**79±7**
GRTP1	**229377_at**	**139±10**	**124±11**	**88±20**	**58±5**
TANC	**225308_s_at**	**760±25**	**722±34**	**470±68**	**427±24**
—	**236766_at**	**57±2**	**62±5**	**37±5**	**31±2**
KIAA1704	**226429_at**	**160±8**	**165±12**	**93±12**	**91±6**
KIAA1002	**203831_at**	**245±12**	**249±10**	**202±19**	**180±5**

ACD, allergic contact dermatitis.
[1]Classification based on annotation and terms defined by the Gene Ontology Consortium
[2]Mean±SE.
[3]Probe sets reporting decreased expression measures at later time points compared with the 0 h time point are typed in bold.

Probe sets defining the elicitation of ACD

One important conclusion from the analysis of both control and patient samples was that there are no signs of genes that are upregulated in the control subjects as a result of the patch test. The gene expression changes occurring in nickel-allergic subjects during the nickel patch test therefore only reflects the

Table 2. Quantitative real-time RT-PCR generally confirms the differential expression for the selected genes

		Expression intensity array versus real-time RT-PCR[1,2]							
		0 h		7 h		48 h		96h	
Gene symbol		Array	RT	Array	RT	Array	RT	Array	RT
SELE	P[4]	38±7	19,584±2,765	41±20	56,760±17,671	447±195	325,111±108,829	654±177	122,641±41,412
	C	29±6	25,554	37±13	30,044±10,926	31±4	25,196	28±7	19,662
IFI30	P	559±39	398,517±47,500	394±26	359,081±26,951	1,057±386	611,160±154,615	1,533±101	834,843±104,921
	C	518±118	317,411	358±25	272,724±36,191	394±45	292,915	454±97	350,157
IL32	P	128±14	2,758,415± 599,274	92±18	2,443,421± 365,419	316±74	5,123,993±1,183,530	391±80	7,202,659±1,870,882
	C	131±17	2,847,666	103±22	2,357,167±777,131	117±17	1,965,779	129±32	2,131,492
CD3D	P	150±21	50,420±5,519	116±13	51,599±6,899	355±104	389,061±220,021	545±109	161,691±41,981
	C	142±52	41,790	97±19	45,264±20,657	108±22	36,131	128±37	30,156
CCL19	P	1,376±221	642,371± 140,322	377±41	265,254±22,906	3,646±1,314	1,537,411± 480,788	3,616±689	1,509,206± 294,681
	C	1,110±256	480,505	418±134	244,181±82,875	613±96	269,448	473±164	304,895
PSMB8[3]	P	284±21	147,209± 59,391	263±13	133,137±39,631	414±55	99,863±35,670	485±21	84,617±21,541
	C	269±72	36,858	264±14	39,538±3,030	308±17	37,521	277±44	40,041
TMSB10	P	5,701±368	3,032,121± 4,57,181	5,776±248	2,633,231± 97,023	7,775±777	3,417,109± 3,31,036	9,228± 640	3,539,319± 421,239
	C	6,764±398	3,170,290	5,625±293	2,601,656± 320,173	5,930±204	2,635,176	6,703±607	3,598,768
BTC[3]	P	46±14	4,797±834	61±9	6,802±2,016	27±9	4,089±882	24±8	2,413±454
	C	132±24	1,712	179±42	1,894±208	148±16	1,152	216±47	1,676
CNTN3	P	40±4	396±103	44±4	368±39	27±5	250±71	26±4	134±20
	C	148±44	1,346	139±28	762±201	121±30	810	152±42	730

RT, reverse transcription.
[1]Mean±SE.
[2]For some of the control samples the SE could not be calculated because too few samples were available.
[3]These genes do not show the expression pattern predicted by the microarray experiment.
[4]P: patients, C: controls.

elicitation of ACD and these changes can accordingly be studied in isolation. A one-way ANOVA of the patient data resulted in the identification of 74 probe sets, which yielded a differential expression measure over time. Cluster analysis revealed that the majority of the probe sets reported an increased expression measure at time point 48 and 96 hours compared to time point 0 and 7 hours (Figure 2). Only the gene expression profile from one sample (the 48 hours biopsy from patient no. 7), did not fit into the described pattern in that it clustered together with the early time-point samples (Figure 2).

In Table 1, the expression levels of all 74 probe sets are given. The gene with the greatest increase in expression (16-fold) in the 48- and 96-hour biopsies compared to the 0- and 7-h our biopsies was granzyme B. Granzyme B is an enzyme necessary for cell lysis in cell-mediated immune responses (Trapani, 2001). Granzyme B was also found upregulated in the DNA microarray study of CHS in the rat (Hartmann *et al.*, 2006). The gene expression profiles of the 0-hour time point were also compared to the 7-hour time point using a Student's *t*-test, but no probe sets were found to report a differential expression measure when using the predefined significance level (false discovery rate $<5\%$). Thus, only minor changes have been induced in the skin transcriptome of an allergic subject 7 hours after exposure to allergen. CCL19 was the only chemokine found to be upregulated (Table 2) using the chosen significance level and we therefore specifically investigated the expression levels for the CCL2, CCL5, CCL17, CCL18, CCL19, CXCL9, and CXCL10, which have previously been demonstrated to be upregulated in the elicitation of ACD by the use of *in situ* hybridization (Goebeler *et al.*, 2001). All of these chemokines were found to be upregulated in the late time points compared to the early time points by at least twofold in our study with a *P*-value below 0.01 for the ANOVA. However, the *q*-value assigned to adjust for multiple tests were above 0.05 and these chemokines were therefore not represented in Table 1.

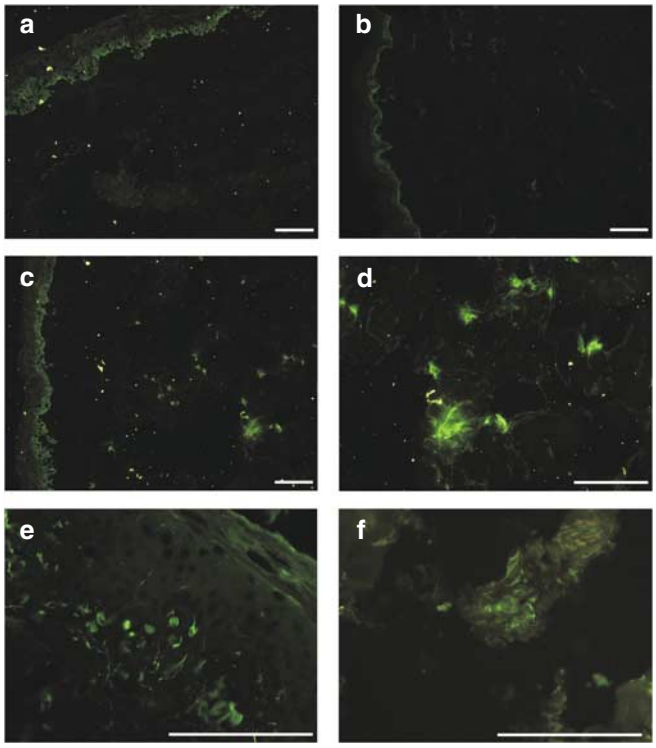

Figure 3. Expression of CCL19 and CCR7 in nickel-exposed skin from allergic subjects. Punch biopsies of 4 mm were taken from a nickel-allergic subject at the time points 0, 7, 48, and 96 hours following the exposure of skin to nickel during a patch test. The biopsies were taken from the skin beneath the patch test. The biopsies from the time points (**a**) 0 hour, (**b**) 7 hours, and (**c** and **d**) 96 hours after nickel exposure were analyzed with a CCL19 antibody. (**c**) At the 96-hour time-point staining deep dermal structures are visible. (**d**) At a higher magnification the staining appears cloudy around cells with an irregular morphology. (**e**) The expression of CCR7 was analyzed in a biopsy from a control subject and (**f**) from an allergic subject 96 hours after nickel exposure. The staining was found in cells scattered in and beneath (**e**) the epidermis and in the dermis. In some areas the CCR7-positive cells were arranged in clusters in (**f**) the deep dermis. Bar = 250 μm.

CCL19 is expressed in deep dermal cells in the late phase of ACD elicitation

To validate the DNA microarray data, the expression of nine genes interrogated by probe sets with differential expression measures was quantified by real-time reverse transcription (RT)-PCR (Table 2). Only two of the genes did not show the expression pattern predicted by the corresponding probe set expression measure. Interestingly, the quantitative real-time RT-PCR analysis also confirmed the upregulation of CCL19 and we investigated if the upregulation of CCL19 might also be confirmed at the protein level using immunocytochemistry. For this purpose a separate biopsy series was obtained from one ACD patient and from one control subject, both of whom were not included in the DNA microarray study. As seen in Figure 3(a–c), weak staining for CCL19 was seen in the basal and suprabasal epidermal cells at the 0-, 7-, and 96-hour time points in the skin from nickel-allergic subjects. The skin from the control subjects showed the same weak epidermal staining (not shown). At the 96-hour time point, scattered points of strong staining were in addition seen in the deeper part of the dermis from the nickel-allergic subject (Figure 3c), but not in the skin from the control subject (not shown). At a higher magnification (Figure 3d), it could be seen that the staining appeared cloudy and diffuse around strongly staining cells. Thus, the staining suggests that CCL19 is released from CCL19-positive cells displaying an irregular morphology. The mRNA for CCR7 was also found to be upregulated at the 48- and 96-hour time points (Table 1). Using a CCR7 antibody, staining was seen in cells scattered in and beneath the epidermis (Figure 3e). This CCR7 staining was seen both in the skin from a control subject and in the skin from the patient at all time points (not shown). In addition, CCR7-positive cells were found scattered deeper in the dermis and in some cases CCR7-positive cells were found in small clusters. These clusters were most easily recognized in the 96-hour patient sample (Figure 3f), but the limited amount of material did not permit a quantitative analysis of the distribution. The 48-hour time-point biopsy from the same series (Figure 3) was divided into fractions by serial sectioning. This allowed the extraction of RNA from fractions representing different regions of the biopsy. Three fractions were produced (Figure 4). The epidermal fraction (fraction 1), the upper dermal fraction (fraction 2), and the deep dermal fraction (fraction 3). Quantitative real-time RT-PCR analysis showed that both the CCL19 and the CCR7 transcripts were only detectable in the deep dermal fraction, whereas control transcripts were detectable in all fractions with highest expression level in either the deep dermal fraction (SELE) or in the epidermal fraction (S100A7), respectively. CCL19 mRNA was, however, detectable by quantitative real-time RT-PCR analysis in the 0 hour biopsies (Table 2), where CCL19 immunostaining was only found in the basal part of the epidermis. The failure to detect CCL19 mRNA by quantitative real-time RT-PCR in the epidermal fraction (Figure 4), therefore, probably reflects the very low amounts of RNA recovered from the tissue sections. Thus only the dermal fractions from the 48-hour biopsy contain sufficient amounts of CCL19 mRNA to allow detection by quantitative real-time RT-PCR. Combined immunocytochemical and quantitative real-time RT-PCR analyses of the biopsy fractions therefore strongly suggest that CCL19 expression is highly upregulated in cells located in the deeper part of the dermis during elicitation of ACD and that this upregulation is accompanied by increased expression of mRNA for CCR7 in the dermis.

DISCUSSION

This study provides early evidence of the global gene expression in the human skin during the elicitation of ACD. Genome-wide gene expression analysis has previously been carried out in nickel-exposed peripheral mononuclear blood cells from nickel allergic subjects (Hansen *et al.*, 2005) and in cultured DCs exposed to dinitrobenzenesulfonic acid (Ryan *et al.*, 2004). Comparisons of the gene expression changes in the skin revealed in this study with those previous reports only resulted in the identification of the chemokine receptor CXCR4, which was also found upregulated in allergen-stimulated DCs (Ryan *et al.*, 2004). The gene expression time

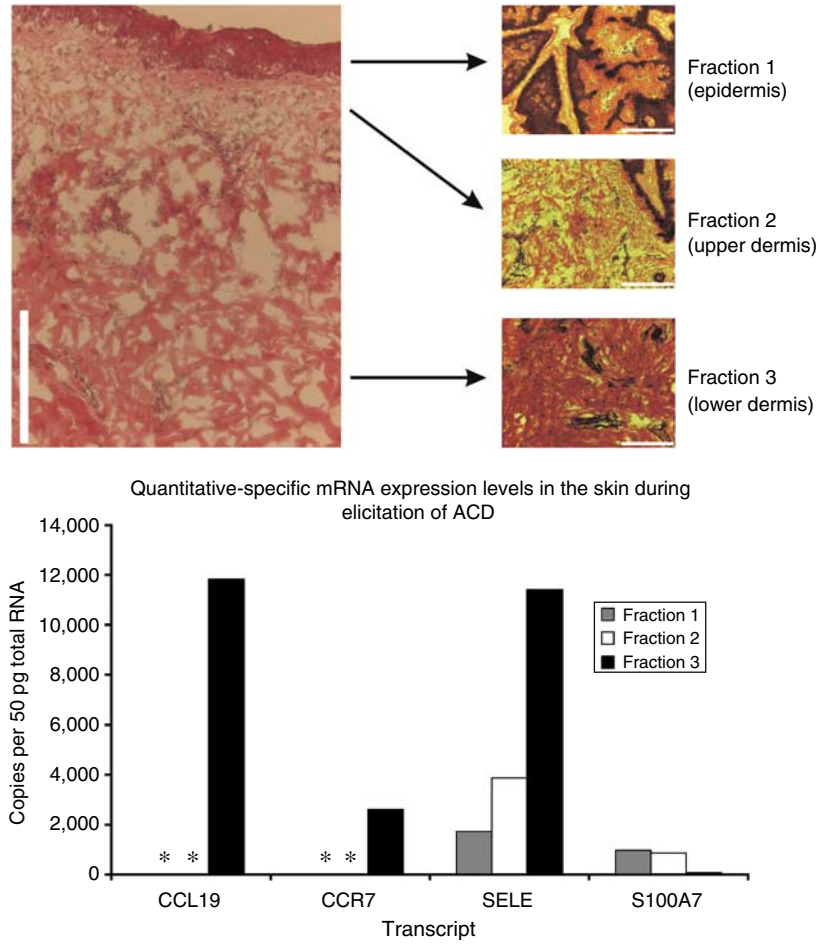

Figure 4. CCL19 mRNA is expressed in the deep dermis beneath the area of nickel exposure during elicitation of ACD. A 4 mm punch biopsy from the 48-hour time point of the time-series experiment shown in Figure 3 was sectioned in parallel to the epidermal surface. The sections were pooled in fractions and RNA extracted. Every tenth section was retained for haematoxylin/eosin staining. The micrograph (bar = 100 μm) on the left is a section from the 96-hour time point. The micrographs (bar = 100 μm) on the right are haematoxylin/eosin-stained sections of the 48-hour biopsy (Figure 3 legend) corresponding to section 10 (700 μm from the surface), section 20 (140 μm from the surface), and section 40 (280 μm from the surface). Sections 1–9 were pooled as fraction 1 (epidermis fraction), sections 11–20 were pooled as fraction 2 (upper dermis fraction), and sections 31–100 were pooled as fraction 3 (lower dermis fraction). RNA was extracted and converted into cDNA. Copy numbers of the indicated transcripts were measured in the fractions by quantitative real-time PCR. The transcript for glyceraldehyde 3-phosphate dehydrogenase was used for normalization. The CCL19 and CCR7 transcripts could not be detected in the fractions 1 and 2 (indicated by asterisks), but were detectable in fraction 3 corresponding to the lower dermis fraction.

course in the skin during elicitation of ACD is therefore very different than the expression changes observed in mononuclear cells or in DCs isolated from peripheral blood. Compared with a study of CHS in the rat (Hartmann *et al.*, 2006), transcripts for STAT1, IRF1, PSMB8, and GRZMB were predicted to be upregulated in both studies.

Potential and unexpected role of CCL19 during the elicitation of ACD

CCL19 and CCL21 are required to elicit an inflammatory response in murine CHS (for reviews see Wang *et al.*, 2003; Ebert *et al.*, 2005). The dogma is, however, that it is the trafficking of T lymphocytes and DCs to the LNs during the sensitization phase, which is defective in these mice. CCL19 and CCL21 are generally referred to as homeostatic chemokines that are constitutively expressed in LNs (Ebert *et al.*, 2005). Our finding of a highly significant upregulated expression of CCL19 in dermal cells during elicitation of ACD suggests that this chemokine and its receptor might also be involved in the elicitation phase. An interesting hypothesis might be that dermally expressed CCL19 recruits and colocalizes CCR7-positive DCs with CCR7-positive T cells directly in the dermis of a sensitized subject. Recently it has been reported that the other CCR7 ligand, CCL21, is expressed in the dermis after irritant exposure and also during elicitation of ACD (Eberhard *et al.*, 2004; Serra *et al.*, 2004). In our gene expression analysis, the CCL21 probe set reported an approximately twofold higher expression measure at the 48-hour time point than at the 0 hour time point with a *P*-value of 0.03. Thus, although this *P*-value did not pass the correction for multiple tests in our DNA microarray experiment, the finding is interesting, supports the upregulation of CCL21 during ACD and might therefore suggest that CCL19 and

CCL21 together cooperate during elicitation of ACD by recruiting CCR7-positive cells to the dermis at the site of hapten exposure.

Functional interpretation of transcriptome changes during elicitation of ACD

The promoter *cis*-element overrepresentation analysis suggests that STAT and SMAD transcription factors might be involved in mediating the transcriptome changes observed during elicitation of ACD. STATs are downstream of γ-interferon signaling that promotes inflammation (for a review see O'neill, 2006). SMADs are downstream of transforming growth factor-β signals that dampen the inflammatory response (for a review see Hanada and Yoshimura, 2002). A straightforward interpretation is that the opposing signaling of the two cytokines is reflected in the late time-point transcriptome data. Whereas the involvement of interferon-γ signaling and the downstream STAT transcription factors was anticipated from the current knowledge (Wang *et al.*, 2003), the overrepresentation of SMAD *cis*-elements in the promoters of genes involved in the elicitation of ACD and the potential involvement of transforming growth factor-β and SMAD signaling was unexpected and worth investigating in future studies.

MATERIALS AND METHODS

Subjects

For the microarray study, seven nickel-allergic patients and five nonallergic controls were recruited. In addition, one nickel-allergic patient and one healthy control were recruited for the immunocytochemistry study. All participants were women and all patients had at least a 2+ reaction to 5% nickel sulfate at the time of diagnosis. The age of the patients ranged from 33 to 49 (mean age 40) and the age of the controls ranged from 31 to 55 (mean age 43). None of the participants used any immunosuppressive medications during the time of the study.

The design and conduct of the skin sampling was in agreement with the declaration of Helsinki Principles. All subjects gave written and informed consent. The study was approved by the Local Ethics Committee.

Allergen exposure and skin biopsies

All patch tests were applied on the upper *nates*. The patch tests were performed using 5% nickel sulfate in pet ($NiSO_4$; Sigma-Aldrich, Broendby, Denmark). The allergen was applied using 8 mm Finn Chambers® (Epitest, Tuusula, Finland) with Scanpor® tape (Norgesplaster, Vennesla, Norway).

All participants were exposed to three patch tests with 5% nickel sulfate: (i) the first patch test was exposed for 7 hours and a skin biopsy was taken immediately after removing the patch test; (ii) the second patch test was exposed for 48 hours immediately followed by a skin biopsy; and (iii) the third patch test was exposed for 48 hours and the skin biopsy was taken 48 hours after removing the patch test (the 96-h biopsy). In addition, all participants were exposed to an empty patch test exposed for 48 hours followed by a skin biopsy. As a result, we obtained four skin biopsies from each participant corresponding to different time points during the development of ACD: 0, 7, 48, and 96 hours. Before taking the skin biopsies (4 mm punch biopsies), the skin was frozen using a liquid nitrogen spray to inhibit RNA degradation. The skin biopsy specimens were immediately placed in liquid nitrogen and were later transferred to a −80°C freezer.

RNA extraction

For RNA extraction, the skin biopsies were placed in a mortar filled with liquid nitrogen and ground mechanically using a pestal. The tissue was transferred to a lysis buffer and RNA was extracted using the RNase Lipid Tissue Kit (Qiagen, Valencia, CA). The amount and quality of the extracted RNA was evaluated using a lab-on-a-chip Bioanalyzer (Agilent Technologies, Santa Clara, CA). Based on the quality of the RNA, a total of 16 control samples and 18 patient samples were found suitable for the microarray experiment, resulting in 3–6 samples per time point for both the patients and the controls. After probe generation for microarray hybridization, sufficient amounts of RNA remained for validation by real-time quantitative RT-PCR from nine control samples and 23 patient samples.

DNA microarrays

Generation of cDNA, biotin-labeled cRNA and GeneChip hybridization was performed by the RH Microarray Centre at Rigshospitalet (Copenhagen, Denmark) as described previously (Hansen *et al.*, 2005). The calculated expression measures and the original data (CEL files) have been submitted to the Gene Expression Omnibus under the accession number GSE6281.

Real-time RT-PCR

Primers for amplification of fragments (between 150 and 250 bp) of the transcripts indicated in Table 2 were chosen from the PrimerBank resource (Wang and Seed, 2003). All amplified PCR products were sequenced to verify the expected identity and melting curves were routinely checked to rule out the amplification of unrelated fragments during quantitative real-time RT-PCR. For the results reported in Table 2 (analysis of whole biopsies), 50 ng of reverse-transcribed total RNA was used as template. For the results reported in Figure 4 (analysis of biopsy fractions), 50 pg of reverse-transcribed total RNA was used as template. The PCR reactions were run using the LightCycler PCR system (Roche, Manheim, Germany). All procedures for the preparation of PCR products for calibration, PCR sequence verification, cDNA synthesis, real-time RT-PCR amplification, and copy number quantification have been described previously (Hansen *et al.*, 2005; Csillag *et al.*, 2007b). The copy numbers for the glyceraldehyde 3-phosphate dehydrogenase transcript were used for normalization between samples.

Immunocytochemistry

Frozen sections of 7 μm were prepared from skin biopsies. The sections were fixed in acetone (4°C) for 10 minutes. The sections were incubated for 30 minutes in blocking buffer (50 mM Tris–HCl (pH 7.4), 150 mM NaCl, 0.5 % ovalbumin, 0.1% gelatine, 0.2% teleostean gelatine, and 0.05 % Tween-20) and incubated (4°C) with a 1:40 dilution of a CCL19 mouse monoclonal antibody (catalog number MAB361, R&D Systems, Abingdon, UK) or CCR7 antibody (catalog number 14-9977-80, eBioscience, San Diego, CA) in blocking buffer overnight. The sections were washed three times for 10 minutes each in blocking buffer and incubated for 30 minutes

at room temperature with a 1:100 dilution of an Alexa-488-conjugated goat anti-mouse antibody (Invitrogen, Carlsbad, CA). After three washes in PBS, the sections were mounted for fluorescence microscopy using DAPI containing Prolong Gold antifade (Invitrogen). One 48-hour patient biopsy was fractionated by serial sectioning in parallel to the epidermis. Details about the fraction collection are given in the legend to Figure 4.

Data analysis

In general, the statistical computations were done using the R environment for statistical computing (for an introduction to R, see Dalgaard, 2002). Summarization of probe level data from the scanned GeneChips into single normalized gene expression measures for each probe set was performed using the robust multiarray analysis procedure with quantile normalization and robust multi-array analysis background correction (Irizarry *et al.*, 2003). A total of eight groups were defined (0, 7, 48, and 96 hours for patients and control subjects) and used in the one-way ANOVA. To deal with multiple tests, a false discovery rate (Storey and Tibshirani, 2003) strategy was applied. The set of *P*-values obtained after performing ANOVA for each probe set were used to calculate *q*-values, and probe sets with *q*-values below 0.0001 were considered significant. CA was performed using the Made4 library (Culhane *et al.*, 2005) for R. The genes contributing the most to the CA axes were extracted from the CA loading matrix as the loadings with values >1 or <1, respectively, for the CA axes. Probe sets with loading values below -1 defined the negative direction of each axis and probe sets with a loading value >1 defined the positive direction of each CA axis. This criterion yielded between 108 and 145 probe sets defining the axes. For each axis the list probe sets with positive loadings and the list of probe sets with negative loadings were analyzed for overrepresented terms for biological processes using the graphical GoSurfer functional annotation analysis tool (Zhong *et al.*, 2004). In addition, the promoters for the genes represented by these probe sets were analyzed for overrepresentation of potential promoter *cis*-elements using PRIMO software (Stegmann *et al.*, 2006) and a set of 65 position weight matrices defining binding sites for vertebrate transcription factors (Stegmann *et al.*, 2006). The obtained *P*-values were corrected for multiple testing by the Bonferroni procedure (Armitage *et al.*, 2002). Three matrices detected overrepresented (M00497, STAT3, 31 promoters with hits and 73 promoters without hits, $P=0.03$; M00470, AP-2γ, 31 promoters with hits, 73 promoters without hits, $P=0.003$; M00792, SMAD, 28 promoters with hits, 76 promoters without hits, $P=0.0003$) *cis*-elements in the promoters defined by the list of probe sets defining the positive direction of the first CA axis. The consensus sequences for the binding sites were as follows: M00497, 5′-G/C G/C A/C TTCC C/G-3′; M00470, 5′-GCC C/T NN GG C/G-3′; M00792, 5′-AGACNCC-3′. The consensus binding sequences for STAT3 and STAT1 are very similar (Park and Schindler, 1998) and the M00497 matrix is not able to distinguish between the two different STAT transcription factors.

To analyze the allergic response in more detail, the patient data were also investigated separately. ANOVA was conducted followed by calculations of *q*-values as described above, except that a significance level of 0.05 for the *q*-value was chosen.

CONFLICT OF INTEREST

The authors state no conflict of interest.

ACKNOWLEDGMENTS

This work was financially supported by the Foundation of Aage Bang, Denmark, The NovoNordic Foundation, the Danish Medical Research Council, The Copenhagen County Research Foundation, and the Alfred Nielsen and Wife's foundation. Ms Liselotte Laustsen is thanked for excellent technical assistance and Ms Susanne Smed from the microarray core facility Rigshospitalet, Copenhagen is thanked for performing GeneChip hybridizations and scannings. The work was performed in Copenhagen, Denmark.

REFERENCES

Armitage P, Berry G, Matthews JNS (2002) *Statistical Methods in Medical Research*. Oxford: Blackwell Science

Ashburner M, Ball CA, Blake JA, Botstein D, Butler H, Cherry JM *et al.* (2000) Gene ontology: tool for the unification of biology. The Gene Ontology Consortium. *Nat Genet* 25:25–9

Csillag C, Nielsen OH, Borup R, Nielsen FC, Olsen J (2007a) Clinical phenotype and gene expression profile in Crohn's disease. *Am J Physiol Gastrointest Liver Physiol* 292:G298–304

Csillag C, Nielsen OH, Vainer B, Olsen J, Dieckgraefe BK, Hendel J *et al.* (2007b) Expression of the genes dual oxidase 2, lipocalin 2, and regenerating islet-derived 1 alpha in Crohn's disease. *Scand J Gastroenterol* 42:454–563

Culhane AC, Thioulouse J, Perriere G, Higgins DG (2005) MADE4: an R package for multivariate analysis of gene expression data. *Bioinformatics* 21:2789–90

Dalgaard P (2002) *Introductory Statistics with R*. New York: Springer-Verlag

Eberhard Y, Ortiz S, Ruiz LA, Kuznitzky R, Serra HM (2004) Up-regulation of the chemokine CCL21 in the skin of subjects exposed to irritants. *BMC Immunol* 5:7

Ebert LM, Schaerli P, Moser B (2005) Chemokine-mediated control of T cell traffic in lymphoid and peripheral tissues. *Mol Immunol* 42:799–809

Goebeler M, Trautmann A, Voss A, Brocker EV, Toksoy A, Gillitzer R (2001) Differential and sequential expression of multiple chemokines during elicitation of allergic contact hypersensitivity. *Am J Pathol* 158:431–40

Hanada T, Yoshimura A (2002) Regulation of cytokine signaling and inflammation. *Cytokine Growth Factor Rev* 13:413–21

Hansen MB, Skov L, Menné T, Olsen J (2005) Gene transcripts as potential diagnostic markers for allergic contact dermatitis. *Contact Dermatitis* 53:100–6

Hartmann B, Staedtler F, Hartmann N, Meingassner J, Firat H (2006) Gene expression profiling of skin and draining lymph nodes of rats affected with cutaneous contact hypersensitivity. *Inflamm Res* 55:322–34

Irizarry RA, Bolstad BM, Collin F, Cope LM, Hobbs B, Speed TP (2003) Summaries of Affymetrix GeneChip probe level data. *Nucleic Acids Res* 31:e15

O'neill LA (2006) Targeting signal transduction as a strategy to treat inflammatory diseases. *Nat Rev Drug Discov* 5:549–63

Park C, Schindler C (1998) Protein–DNA interactions in interferon-gamma signaling. *Methods* 15:175–88

Rustemeyer T, van Hoogstraten IM, von Blomberg BME, Scheper RJ (2003) Mechanisms in allergic contact dermatitis. In: Frosh PJ, Menné T, Lepoittevin J-P (eds) *Contact Dermatitis*. Berlin Heidelberg: Springer-Verlag, pp 11–43

Ryan CA, Gildea LA, Hulette BC, Dearman RJ, Kimber I, Gerberick GF (2004) Gene expression changes in peripheral blood-derived dendritic cells following exposure to a contact allergen. *Toxicol Lett* 150:301–16

Sanchez-Sanchez N, Riol-Blanco L, Rodriguez-Fernandez JL (2006) The multiple personalities of the chemokine receptor CCR7 in dendritic cells. *J Immunol* 176:5153–9

Scheynius S (1998) Immunological aspects In: Lepoittevin J-P, Basketter DA, Goossens A, Karlberg AT (eds) *Allergic Contact Dermatitis – The Molecular Basis*. Berlin Heidelberg: Springer-Verlag, pp 4–18

Sebastiani S, Albanesi C, De PO, Puddu P, Cavani A, Girolomoni G (2002) The role of chemokines in allergic contact dermatitis. *Arch Dermatol Res* 293:552–9

Serra HM, Eberhard Y, Martin AP, Gallino N, Gagliardi J, Baena-Cagnani CE *et al.* (2004) Secondary lymphoid tissue chemokine (CCL21) is upregulated in allergic contact dermatitis. *Int Arch Allergy Immunol* 133:64–71

Stegmann A, Hansen M, Wang Y, Larsen JB, Lund LR, Ritié L *et al.* (2006) Metabolome, transcriptome and bioinformatic *cis*-element analyses point to HNF-4 as a central regulator of gene expression during enterocyte differentiation. *Physiol Genomics* 27: 141–55

Storey JD, Tibshirani R (2003) Statistical significance for genomewide studies. *Proc Natl Acad Sci USA* 100:9440–5

Stoughton RB (2005) Applications of DNA microarrays in biology. *Annu Rev Biochem* 74:53–82

Trapani JA (2001) Granzymes: a family of lymphocyte granule serine proteases. *Genome Biol* 2: REVIEWS3014.1–3014.7

Veien NK (2006) Clinical features: General aspects In: Frosh PJ, Menné T, Lepoittevin J-P (eds) *Contact Dermatitis*. Berlin Heidelberg: Springer-Verlag, pp 201–54

Wang B, Esche C, Mamelak A, Freed I, Watanabe H, Sauder DN (2003) Cytokine knockouts in contact hypersensitivity research. *Cytokine Growth Factor Rev* 14:381–9

Wang X, Seed B (2003) A PCR primer bank for quantitative gene expression analysis. *Nucleic Acids Res* 31:e154

Zhong S, Storch KF, Lipan O, Kao MC, Weitz CJ, Wong WH (2004) GoSurfer: a graphical interactive tool for comparative analysis of large gene sets in Gene Ontology space. *Appl Bioinformatics* 3:261–4